Journal of Power Sources 213 (2012) 304–316

Contents lists available at SciVerse ScienceDirect

Journal of Power Sources

journal homepage: www.elsevier.com/locate/jpowsour

Reinvestigation on the state-of-the-art nonaqueous carbonate electrolytes for 5 V Li-ion battery applications

Wu Xu [a,*,1], Xilin Chen [a,1], Fei Ding [a,b], Jie Xiao [a], Deyu Wang [a,2], Anqiang Pan [a,3], Jianming Zheng [a], Xiaohong S. Li [a], Asanga B. Padmaperuma [a], Ji-Guang Zhang [a,**]

[a] Energy and Environment Directorate, Pacific Northwest National Laboratory, Richland, WA 99354, USA
[b] National Key Laboratory of Power Sources, Tianjin Institute of Power Sources, Tianjin 300381, PR China

ARTICLE INFO

Article history:
Received 28 February 2012
Received in revised form
30 March 2012
Accepted 16 April 2012
Available online 25 April 2012

Keywords:
Li-ion battery
Electrolyte
Carbonate solvent
Oxidation potential
High voltage

ABSTRACT

The charging voltage limits of mixed-carbonate solvents for Li-ion batteries were systematically investigated from 4.9 to 5.3 V in half-cells using Cr-doped spinel cathode material $LiNi_{0.45}Cr_{0.05}Mn_{1.5}O_4$. The stability of conventional carbonate electrolytes is strongly related to the stability and properties of the cathode materials in the de-lithiated state. This is the first time report that the conventional electrolytes based on mixtures of EC and linear carbonate (DMC, EMC and DEC) can be cycled up to 5.2 V on $LiNi_{0.45}Cr_{0.05}Mn_{1.5}O_4$ for long-term cycling, where their performances are similar. The discharge capacity increases with the charging cutoff voltage and reaches the highest discharge capacity at 5.2 V. The capacity retention is about 87% after 500 cycles at 1C rate for all three carbonate mixtures in half-cells when cycled between 3.0 V and 5.2 V. When cycled to 5.3 V, EC-DMC still shows good cycling performance but EC-EMC and EC-DEC show faster capacity fading. EC-DMC and EC-EMC have much better rate capability than EC-DEC. The first-cycle irreversible capacity loss increases with the cutoff voltage. The "inactive" conductive carbon is also partly associated with the low first-cycle Coulombic efficiency at high voltages due to electrolyte decomposition and possible PF_6^- anion irreversible intercalation.

1. Introduction

The state-of-the-art (SOA) Li-ion batteries have achieved great success in portable electronics and power tools. They are now starting to enter the electric vehicle (EV) and grid energy storage markets. For EV applications, the SOA Li-ion battery technology can only meet the requirements for short-range applications due to their limited energy density. To further improve the energy density of a Li-ion battery, cathode and anode materials with higher specific capacities and cathode materials with a higher voltage plateau are required. Some 5 V cathode materials have shown very promising results to enhance the energy density of Li-ion batteries, which include $Li_3V_2(PO_4)_3$ (charged to 4.8 V) [1,2], $LiNi_{0.5}Mn_{1.5}O_4$ and its doped derivatives (4.9 V) [3–10], $LiCoPO_4$ (5.0 V) [11–13], Li_2CoPO_4F (5.5 V) [14,15], and others. However, the high voltage stability of the electrolytes has always been one of the main barriers to the application of these high operating voltage materials.

Previous literature indicates much confusion on the upper voltage limits of the SOA Li-ion battery electrolytes based on organic carbonate solvents. For example, it has been reported that the carbonate electrolytes are not stable at 4.3–4.5 V vs. Li/Li^+ on $LiCoO_2$ and $LiNi_xMn_yCo_zO_2$ (where $x + y + z = 1$) electrodes [16–20]. However, some of the carbonate electrolytes exhibit very good battery performance when used for $LiNi_{0.5}Mn_{1.5}O_4$ materials in the voltage range up to 4.9 V [8,9,21,22]. Therefore, it is necessary to re-evaluate the carbonate-based nonaqueous electrolytes for high voltage Li-ion batteries to clarify the issue. In this work we report our recent findings on the oxidation potential limits of carbonate-based electrolytes when used with Cr-doped $LiNi_{0.5}Mn_{1.5}O_4$ cathode material ($LiCr_{0.05}Ni_{0.45}Mn_{1.5}O_4$). The electrochemical stability and performance of this battery system will also be reported.

* Corresponding author. Tel.: +1 509 375 6934; fax: +1 509 375 3864.
** Corresponding author. Tel.: +1 509 372 6515; fax: +1 509 375 3864.
E-mail addresses: wu.xu@pnnl.gov (W. Xu), jiguang.zhang@pnnl.gov (J.-G. Zhang).
[1] These authors contributed equally to this work.
[2] Present address: Ningbo Institute of Material Technology and Engineering, Chinese Academy of Sciences, No. 519 Zhuangshi Road, Zhenhai District, Ningbo, Zhejiang 315201, China.
[3] Present address: School of Chemical and Biomedical Engineering, Nanyang Technological University, 70 Nanyang Drive, Singapore.

0378-7753/$ – see front matter © 2012 Elsevier B.V. All rights reserved.
doi:10.1016/j.jpowsour.2012.04.031

2. Experimental

2.1. Electrolyte and electrode preparation

Battery-grade ethylene carbonate (EC), propylene carbonate (PC), dimethyl carbonate (DMC), ethyl methyl carbonate (EMC), diethyl carbonate (DEC), and lithium hexafluorophosphate ($LiPF_6$) were purchased from Novolyte Technologies. Lithium foil (0.75 mm thick) was purchased from Alfa Aesar. All chemicals and materials were used as received. Electrolytes of 1.0 M $LiPF_6$ in single-carbonate solvents and carbonate mixtures (EC-EMC, EC-DEC, EC-DMC, all in 3:7 volume ratio) were prepared in an MBraun glove box filled with purified argon.

$LiCr_{0.05}Ni_{0.45}Mn_{1.5}O_4$ was synthesized by ball milling a mixture of Li_2CO_3, NiO, Cr_2O_3 and $MnCO_3$ (all from Sigma–Aldrich) in stoichiometric amounts for 4 h followed by a heat treatment at 900 °C for 24 h in air and a further annealing at 700 °C for 8 h. Details on the preparation and characterization of this material were reported elsewhere [23]. A slurry of $LiCr_{0.05}Ni_{0.45}Mn_{1.5}O_4$, Super P® conductive carbon black (SP, from Timcal), and polyvinylidene fluoride (PVDF, Kynar HSV900, from Arkema Inc.) in an *N*-methyl pyrrolidone (NMP, from Aldrich) solvent was prepared and cast onto an aluminum foil (from All Foils, Inc.). The weight ratio of $LiCr_{0.05}Ni_{0.45}Mn_{1.5}O_4$:SP:PVDF was 8:1:1 and the active material loading was ~4 mg cm^{-2}. After evaporating the NMP, the cathode sheet was pressed at 3000 psi for 1 min, die-cut into disks with a diameter of 1.27 cm, dried at 110 °C under vacuum overnight, and stored in the glove box. For comparison, an electrode sheet of SP-PVDF (1:1 by wt) was also prepared using the same procedures.

2.2. Characterization and computation

The viscosity and ionic conductivity of the electrolytes at room temperature were measured according to previously reported procedures [24]. The viscosity measurement was conducted on a Brookfield DV-II+ Pro Cone/Plate Viscometer at a spindle speed of 10 rpm. The conductivity was measured using an Oakton® 650 Series Multiparameter Meter. Before tests, all instruments were calibrated and the electrolytes were maintained at 25 °C in a constant-temperature oil bath (Brookfield Circulating Bath Model TC-502).

The surface areas of the electrodes were determined by the Brunauer-Emmett-Teller (BET) method, using nitrogen adsorption/desorption collected with a Quantachrome Autosorb 6-B gas sorption system on degassed samples, as described in a previous report [25]. The as-prepared electrodes were placed in a Macrocell (18 × 40 mm sample holder for large sample pieces) and degassed at 25 °C overnight under vacuum. The degassed samples were tested by nitrogen adsorption/desorption at a constant temperature of 77.4 K. The volume of N_2 gas that adsorbed unto/desorbed from the surface of samples was measured (isothermally) vs. relative pressure. The surface area was determined from the isotherm using a five-point BET method.

The highest occupied molecular orbital (HOMO) energies were calculated from the optimized geometry via density functional theory using the Becke, 3-parameter, Lee-Yang-Parr hybrid functionals [26–30]. The calculations were performed with the NWChem computational package as reported previously [31]. The selected level of theory represents a good compromise between computational efficiency and accuracy for the study of ground state geometries.

2.3. Electrochemical tests

The electrochemical oxidation stabilities of liquid electrolytes on different substrates were screened by linear sweep voltammetry (LSV) in a beaker cell (inside the glove box) composed of three electrodes. Li metal was used as both reference and counter electrodes. The electrolyte samples on different working electrodes were scanned from the open circle voltage to 6.5 V vs. Li/Li^+ at a scan rate of 0.1 mV s^{-1} using a CHI 660C electrochemical workstation (CH Instruments). The cyclic voltammetry (CV) of the $LiCr_{0.05}Ni_{0.45}Mn_{1.5}O_4$ electrode in three electrolytes of conventional carbonate mixtures was tested on a CHI 1000A electrochemical station (CH Instruments) using Li metal as counter electrode. The samples were scanned between 3 V and different cutoff voltages from 4.9 to 5.3 V at a scan rate of 10 μV s^{-1}. All the electrochemical tests were operated at room temperature.

Coin cell kits of CR2032 type were purchased from MTI Corporation. The negative covers, spacers and springs were made of stainless steel 316 (SS-316), and the positive containers were Al-clad SS-316. Whatman® glass fiber B (GF/B) paper with a diameter of 1.91 cm was used as the separator since it has been reported to be stable at high voltages and has no wetting issues with electrolytes containing single cyclic carbonate solvents and EC-DMC mixture [15]. $Li/LiCr_{0.05}Ni_{0.45}Mn_{1.5}O_4$ half-cells with excess electrolyte were assembled on an electric coin cell crimper (from MTI) inside the glove box. The cells were cycled between 3.0 V and different cutoff voltages from 4.9 to 5.3 V at different current rates on Arbin BT-2000 Battery Testers.

3. Results and discussion

3.1. Conductivity and voltammetric behavior of carbonate electrolytes

The SOA nonaqueous electrolytes for Li-ion batteries contain mixtures of cyclic carbonate (EC, PC) and linear carbonates (DMC, EMC, DEC, and so on) for a wide liquid region, low viscosity and high conductivity. The viscosity and ionic conductivity data for the electrolytes of 1.0 M $LiPF_6$ in single- and mixed-carbonate solvents are summarized in Table 1, along with the HOMO energies of the single-carbonate solvents. The apparent ionic conductivity of the electrolyte is related to the reverse effects of the viscosity of the solution and the number of free ions that is associated with the solvent polarity. The electrolyte of 1.0 M $LiPF_6$ in EC has the highest conductivity among the single-carbonate solvents because EC has the highest polarity (dielectric constant of 89.8). The electrolyte of DMC has higher conductivity than that of PC, which is mainly attributed to the much lower viscosity of DMC electrolyte. The electrolytes of 1.0 M $LiPF_6$ in mixed carbonates of EC and linear carbonates, in descending order of conductivity, are EC-DMC > EC-EMC > EC-DEC.

The electrochemical oxidation potentials of these electrolytes have been studied previously on smooth, inert metal (e.g. Pt) and glassy carbon electrodes as well as some real active cathode

Table 1
HOMO energies and physical properties of single-carbonate solvents.

Carbonate	HOMO energy (eV)	1.0 M $LiPF_6$ solution	
		Conductivity at 25.0 °C (mS cm^{-1})	Viscosity at 24.7 °C (cP)
EC	−7.70	8.27	7.74
PC	−7.63	5.65	9.18
DMC	−7.80	6.78	1.20
EMC	−7.30	4.27	2.04
DEC	−7.25	2.87	2.76
EC-DMC[a]	N. A.	11.76	2.64
EC-EMC[a]	N. A.	9.13	4.32
EC-DEC[a]	N. A.	6.90	4.02

[a] Note: The volume ratio of EC to linear carbonate (DMC, EMC or DEC) is 3:7.

materials [16–20]. In this work, we first compared the electrochemical oxidation potentials of the electrolytes from each single-carbonate solvent on different electrodes (Pt, Al, SP-PVDF, and $LiCr_{0.05}Ni_{0.45}Mn_{1.5}O_4$-SP-PVDF), then compared the electrochemical oxidation potentials of three most commonly used carbonate mixtures (EC-DMC, EC-EMC and EC-DEC) on these electrodes. The single solvent DEC was not tested because it reacts quickly with Li metal, which was used as reference and counter electrodes in the LSV tests. As is well known, the current in LSV tests is proportional to the surface area; thus the current density has been normalized by the actual BET surface area of the working electrode to provide relatively fair comparison (this is only an approximation because some of the BET area may not be active). The BET surface areas of SP-PVDF and $LiCr_{0.05}Ni_{0.45}Mn_{1.5}O_4$-SP-PVDF were 2.1 and 3.4 $m^2\ g^{-1}$, respectively.

The oxidation potential on Pt for the single-carbonate solvents has the following order: DMC (5.0 V) > EC (4.8 V) ~ PC (4.8 V) > EMC (4.6 V), as shown in Fig. 1(a). This is consistent with the HOMO energies of these carbonate solvents as shown in Table 1. A higher value of the absolute HOMO energy indicates a higher oxidation potential of the solvent. However, when the cyclic carbonate and linear carbonate solvents are mixed, for example, EC with three linear carbonates in this work, the oxidation potentials of the mixtures are slightly increased compared to the single solvent (Fig. 1(b)), reaching 5.1 V for EC-DMC, 4.9 V for EC-EMC, and 5.0 V for EC-DEC. This is probably due to the synergistic effect of the cyclic and linear carbonate co-solvents.

In practical Li-ion batteries, the cathodes are prepared by coating the mixture of active cathode material with conductive carbon and polymer binder onto both sides of an Al foil. The active materials are normally particles of micro or even nano sizes with high surface areas. In addition, conductive carbon such as SP also has a relatively high surface area of about 60 $m^2\ g^{-1}$. To distinguish the effects of different electrode components on the oxidation potentials of electrolytes, the above LSV measurements were repeated using Al substrate (Fig. 1(c) and (d)), SP-PVDF on Al substrate (Fig. 1(e) and (d)), and $LiCr_{0.05}Ni_{0.45}Mn_{1.5}O_4$-SP-PVDF on Al substrate (Fig. 1(g) and (h)).

It is seen from Fig. 1(c) and (d) that the electrochemical oxidation currents of all tested electrolytes on Al foil are extremely low (less than 1 $\mu A\ cm^{-2}$) as compared with the results obtained on Pt substrate. The high current densities of Pt can be attributed to the catalytic effect of Pt on the decomposition of the electrolytes. It demonstrates that the carbonate solvents are quite stable on Al even up to 6.5 V vs. Li/Li^+, which is probably because of the good protection by the thin and dense alumina film on the Al surface.

When the SP-PVDF on Al was used as the working electrode, the single carbonates had oxidation potentials of 4.8 V for EC and DMC, 4.7 V for PC, and 4.6 V for EMC (see Fig. 1(e)) while the mixed carbonates (EC-DMC, EC-EMC, and EC-DEC) have nearly the same oxidation potential of 4.8 V (as shown in Fig. 1(f)). It should be noted that the electrochemical reactions occurring on the SP-PVDF electrode include the electrolyte oxidation on the relatively high surface area carbon SP and the intercalation of anions into the conductive carbon when the voltage is above 4.5 V as reported previously [32–36].

The LSV curves of the practical electrode ($LiCr_{0.05}Ni_{0.45}Mn_{1.5}O_4$-SP-PVDF on Al substrate) in the electrolytes with single carbonates and mixed carbonates are shown in Fig. 1(g) and Fig. 1(h), respectively. Three oxidation peaks at about 4.1, 4.7 and 4.8 V vs. Li/Li^+ are found in Fig. 1(g) and (h) before a significant current increase related to the electrolyte decomposition occurs. These peaks can be attributed to the oxidation of Mn^{3+} to Mn^{4+} (ca. 4.1 V), Ni^{2+} to Ni^{3+} (ca. 4.7 V) and Ni^{3+} to Ni^{4+} (ca. 4.8 V). We also notice that EC is stable up to 6.5 V even when used with the practical cathode. However, it cannot be used independently in Li-ion batteries because the Li salt-EC electrolytes easily solidify at ambient or sub-ambient temperatures.

Fig. 1(g) and (h) indicate that the electrolyte decomposition becomes more evident on the practical cathode as compared with the results obtained on Al (Fig. 1(c) and (d)) and SP-PVDF (Fig. 1(e) and (f)), especially when the voltage is increased to more than 5.4 V. This relative larger instability can be ascribed to the high surface area of the practical cathode and the anion intercalation into the conductive carbon. It is also noticed from Fig. 1(g) that the single-carbonate solvents do have some difference in electrochemical stability (in the order of EC ~ PC (ca. 5.3 V) > DMC ~ EMC (ca. 5.1 V)) when tested with the $LiCr_{0.05}Ni_{0.45}Mn_{1.5}O_4$ electrode, indicating that the cyclic carbonates are slightly more stable than linear carbonates. However, all the mixed-carbonate solvents have similar oxidation behavior when the voltage is lower than 5.3 V. This indicates that EC plays an important role in the stability of the electrolyte at voltages up to 5.3 V. Therefore, more detailed studies have been performed on the high voltage (up to 5.3 V) performances of the $LiNi_{0.45}Cr_{0.05}Mn_{1.5}O_4$ cathode using the electrolytes with three carbonate mixtures (EC-DMC, EC-EMC and EC-DEC).

Figs. 2–4 show the CV curves of the $LiNi_{0.45}Cr_{0.05}Mn_{1.5}O_4$ cathode using the electrolytes containing the aforementioned carbonate mixtures of (a) EC-DMC, (b) EC-EMC and (c) EC-DEC, respectively. The samples were scanned in the voltage range from 3.5 V to different cutoffs up to 5.3 V at a slow scan rate of 10 $\mu V\ s^{-1}$. All CV curves show three pairs of redox couples: one small but broad redox peak at about 4.0 V for Mn^{3+}/Mn^{4+} and two large, sharp redox peaks at around 4.7 V for Ni^{2+}/Ni^{4+} of the $LiNi_{0.5}Mn_{1.5}O_4$ cathode materials [4,37–43]. When the upper cutoff voltage is set at 5.0 V and up to 5.3 V (the figures (b) to (e) in Figs. 2–4), a fourth pair of redox peaks at about 4.85 V is observed, which is ascribed to the Cr^{3+}/Cr^{4+} redox couple. This pair of redox peaks is not obvious when the upper cutoff voltage is 4.9 V (the figure (a) in all three cases). It indicates that the doped Cr is actually electrochemically active and reversible when the cutoff voltage is higher than 4.9 V.

It is also seen from Figs. 2–4 that the three carbonate mixtures do not show obvious oxidation currents related to electrolyte decomposition when the upper cutoff voltage is lower than 5.2 V. However, the CV curves do show a little oxidation of electrolyte in the first anodic scan when the voltage is cut at 5.3 V. These results indicate that the three carbonate mixtures are quite stable up to 5.2 V.

3.2. Charge-discharge performance

Fig. 5 shows the charge-discharge curves of the half-cells of $Li/LiCr_{0.05}Ni_{0.45}Mn_{1.5}O_4$ using (a) EC-DMC, (b) EC-EMC and (c) EC-DEC as electrolyte solvent, respectively. The voltage plateaus shown in these figures are consistent with the CV scan peaks shown in Figs. 2–4. However, no obvious plateaus but slight slopes are observed corresponding to the Cr^{3+}/Cr^{4+} redox couple.

The variation of the first-cycle Coulombic efficiency with charge cutoff voltage for the three carbonate mixtures is depicted in Fig. 6. Each efficiency data point is an average value from three to four parallel cells. Obviously, the three carbonate mixtures show similar first-cycle efficiency. That is, the efficiency increases slightly when the charge voltage increases from 4.9 V to 5.1 V and then drops when the charge voltage further increases, showing a maximum efficiency at 5.1 V. This phenomenon can be explained by the balance of the contrary effects of increases in the reversible capacity and the irreversible capacity loss with the increase of charge voltage limit. In this case, The Coulombic efficiency, *Eff* can be calculated by

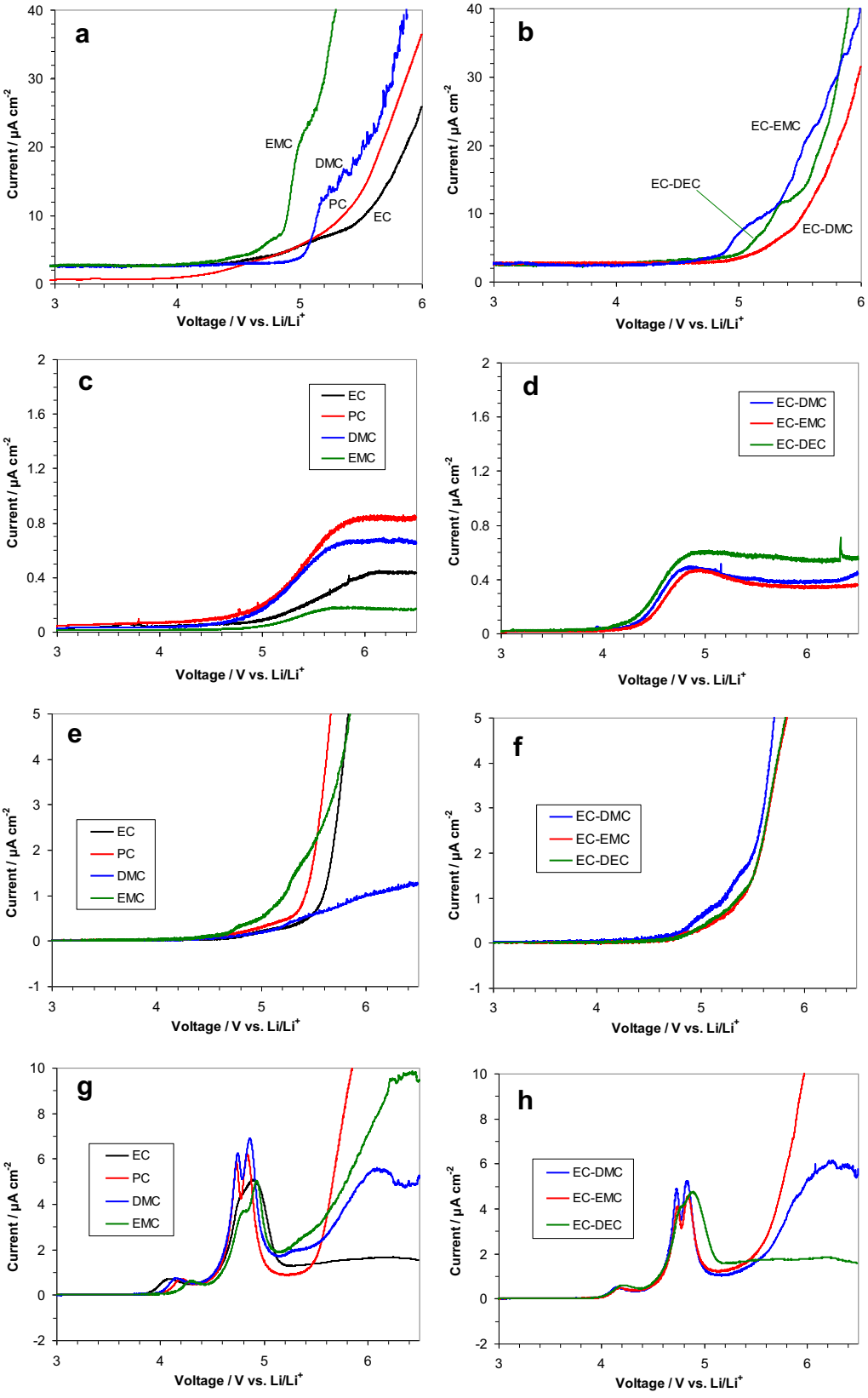

Fig. 1. LSV curves of half-cells using electrolytes of 1.0 M $LiPF_6$ in carbonate solvents at a scan rate of 0.1 mV s^{-1}. The working electrodes used in the half-cells are: Pt (a, b), Al (c, d), SP-PVDF (e, f), and $LiCr_{0.05}Ni_{0.45}Mn_{1.5}O_4$-SP-PVDF (g, h).

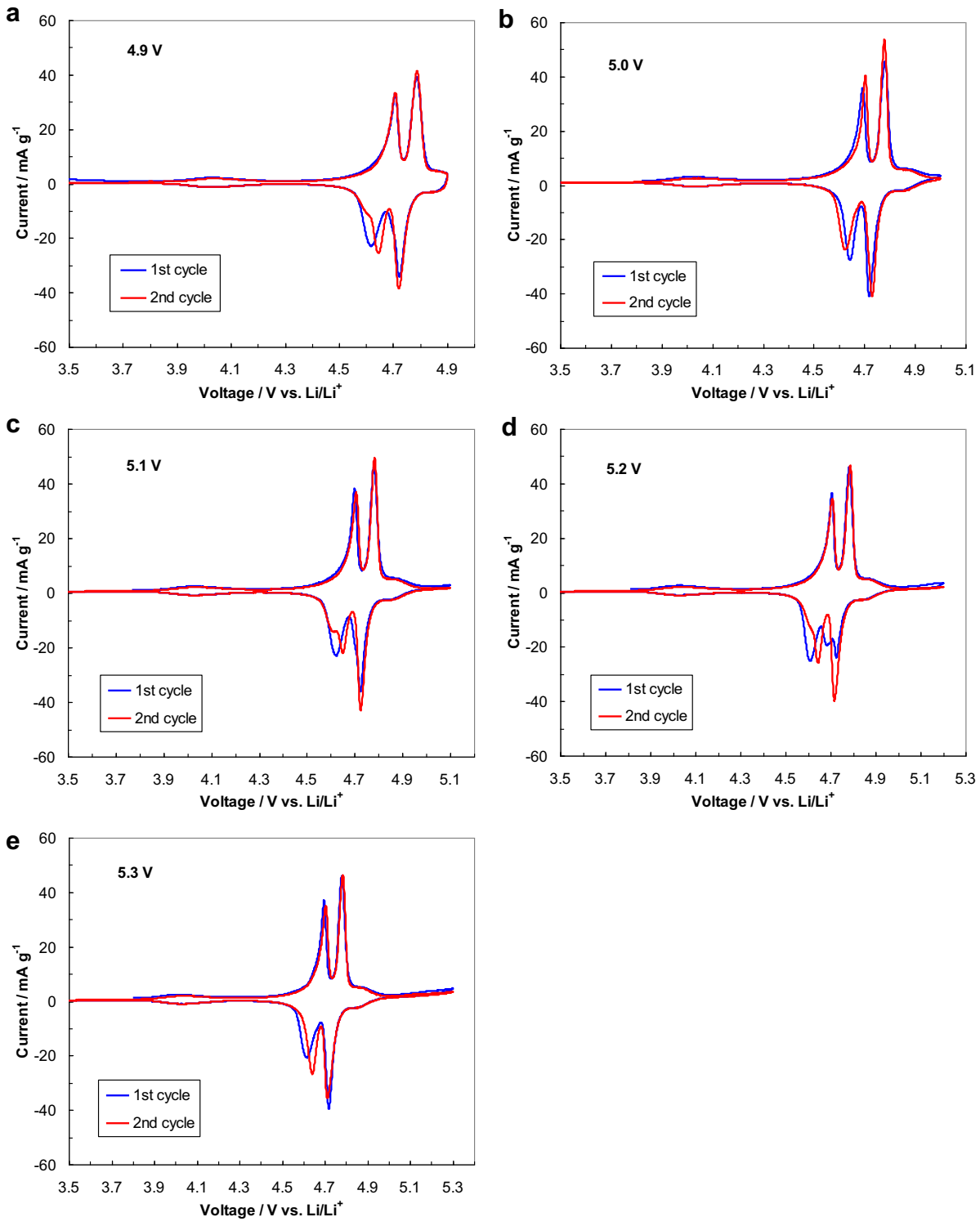

Fig. 2. CV curves of $Li/LiCr_{0.05}Ni_{0.45}Mn_{1.5}O_4$ half-cells with electrolytes of 1.0 M $LiPF_6$ in EC-DMC mixture in the voltage ranges from 3.5 V to (a) 4.9 V, (b) 5.0 V, (c) 5.1 V, (d) 5.2 V, and (e) 5.3 V at a scan rate of 10 μV s^{-1}.

$$Eff = \frac{C_{re}}{C_{re} + C_{irr}} = \frac{1}{1 + C_{irr}/C_{re}}$$

where C_{re} is the reversible capacity and C_{irr} is the irreversible capacity. As discussed previously, the increase of the cutoff voltage limit activates the Cr^{3+}/Cr^{4+} redox couple and the extra Ni^{2+}/Ni^{4+} redox couple, which in turn increases the reversible capacity and the Coulombic efficiency. However, the electrolyte decomposition on the cathode, especially on the surface of conductive carbon, significantly increases with the increasing cutoff voltage limit (see Fig. 7). This will increase the irreversible capacity loss and then lead to decreased Coulombic efficiency. These contrary effects result in an ambiguous maximum Coulombic efficiency at about 5.1 V.

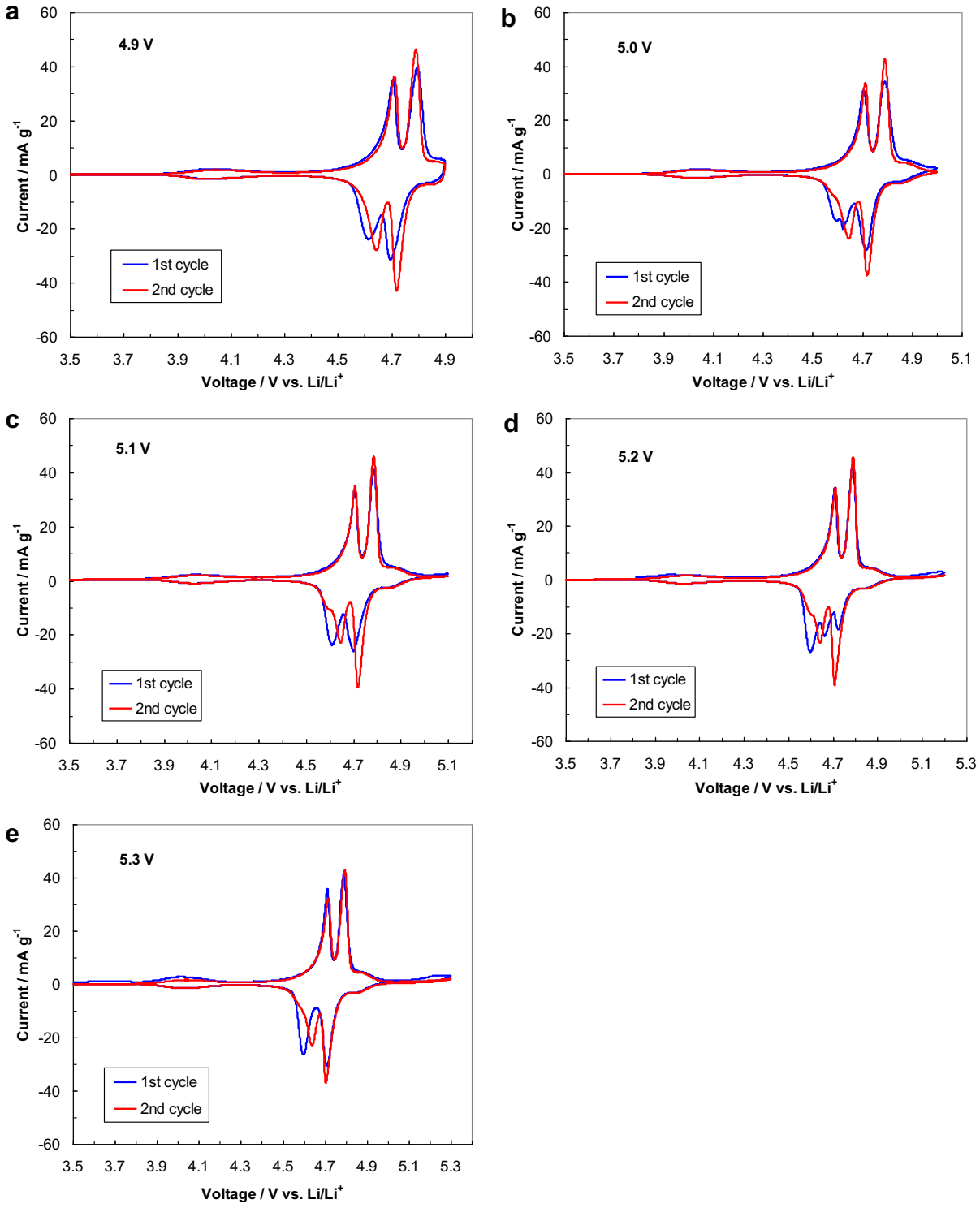

Fig. 3. CV curves of Li/$LiCr_{0.05}Ni_{0.45}Mn_{1.5}O_4$ half-cells with electrolytes of 1.0 M $LiPF_6$ in EC-EMC mixture in the voltage ranges from 3.5 V to (a) 4.9 V, (b) 5.0 V, (c) 5.1 V, (d) 5.2 V, and (e) 5.3 V at a scan rate of 10 μV s^{-1}.

The discharge capacities during long-term cycling (up to 500 cycles) in half-cells at room temperature for the three carbonate mixtures at different upper cutoff voltages are shown in Fig. 8 and compared in Fig. 9. The discharge capacity retentions are compared in Fig. 10 for easy observation. All the cells were cycled at the C/10 rate (1C = 147 mAh g^{-1}) for the first two cycles and then at the 1C rate for the rest of the cycles. The discharge capacity and capacity retention of $LiCr_{0.05}Ni_{0.45}Mn_{1.5}O_4$ increases with the cutoff voltage from 4.9 V to 5.2 for all the three carbonate mixtures. However, when the upper cutoff voltage is set at 5.3 V, the samples with EC-DMC solvent continue to show a little increased capacity and almost the same capacity retention after 500 cycles in comparison

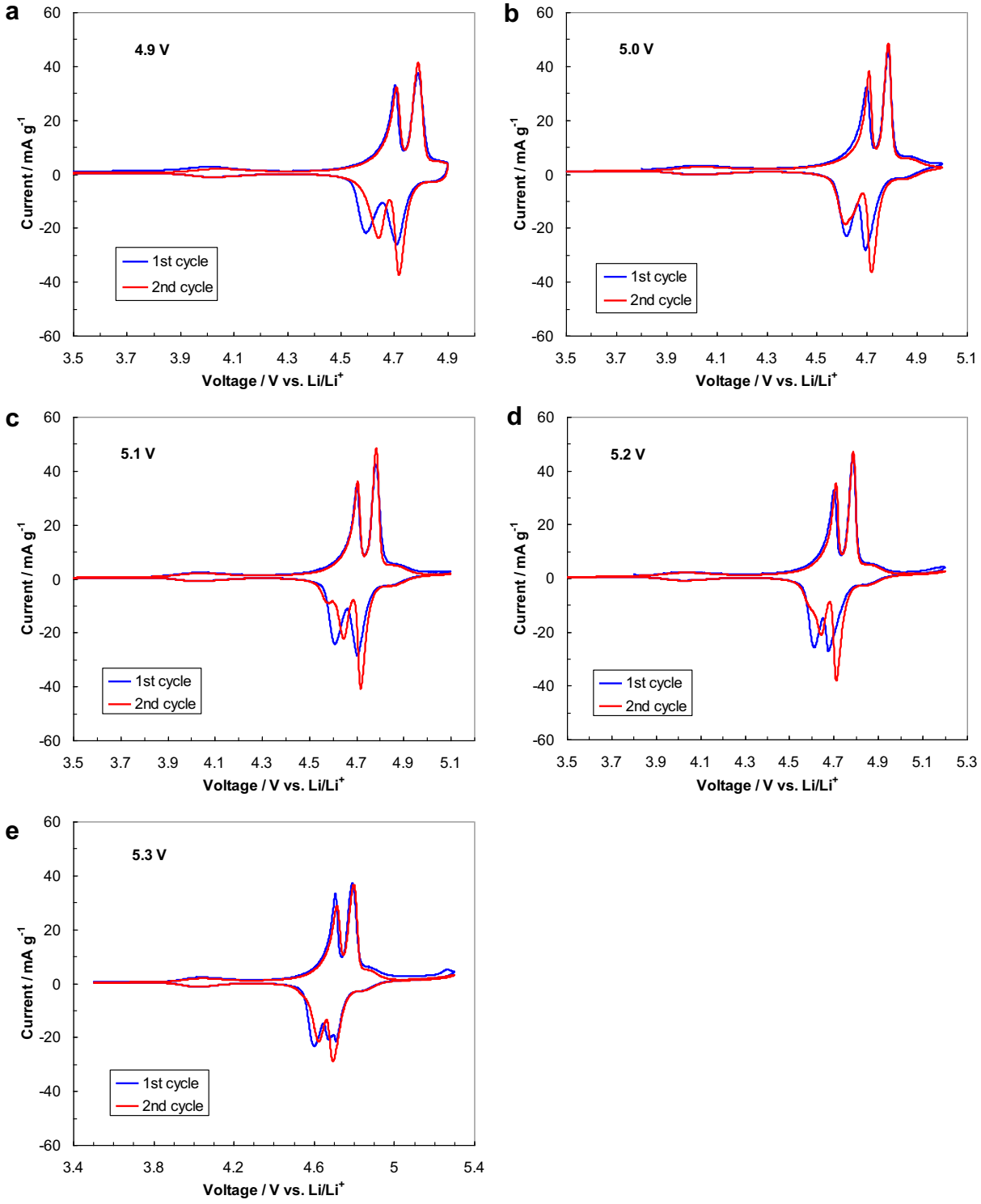

Fig. 4. CV curves of Li/$LiCr_{0.05}Ni_{0.45}Mn_{1.5}O_4$ half-cells with electrolytes of 1.0 M $LiPF_6$ in EC-DEC mixture in the voltage ranges from 3.5 V to (a) 4.9 V, (b) 5.0 V, (c) 5.1 V, (d) 5.2 V, and (e) 5.3 V at a scan rate of 10 μV s^{-1}.

with the samples with a cutoff voltage of 5.2 V. The samples with EC-EMC solvent cycled at 5.3 V show slightly higher capacity than the 5.2 V cells in the first 400 cycles but lower capacity at the 500th cycle, while EC-DEC at 5.3 V shows lower capacity than the 5.2 V cells after 100 cycles. The reasons are explained below.

The active cathode material $LiCr_{0.05}Ni_{0.45}Mn_{1.5}O_4$ has major voltage profiles at 4.66 and 4.76 V during charge and 4.74 and 4.65 V during discharge. Due to the cell internal resistances, the polarization at the 1C rate cannot be ignored. When the charge voltage limit is set to 4.9 V, the Li^+ ions in the active material are actually not completely de-intercalated due to the polarization. When the charge voltage limit is increased from 4.9 V to 5.2 V, more Li^+ ions are withdrawn from the cathode material during charge, and then more Li^+ ions can be re-intercalated into the active

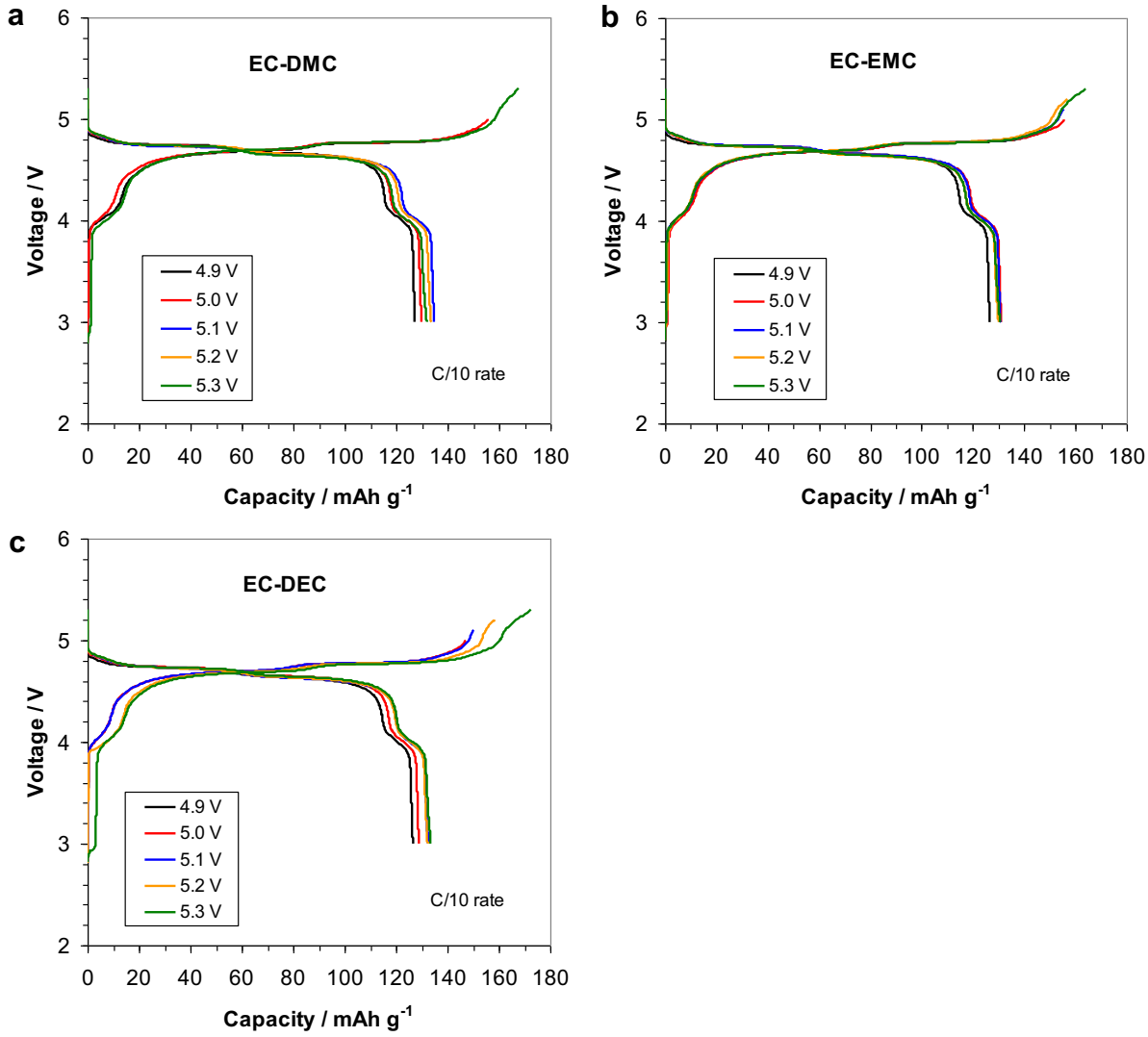

Fig. 5. First cycle charge-discharge curves of Li/$LiCr_{0.05}Ni_{0.45}Mn_{1.5}O_4$ half-cells at different charge cutoff voltages using electrolytes of 1.0 M $LiPF_6$ in (a) EC-DMC, (b) EC-EMC and (c) EC-DEC.

material during subsequent discharge due to the excellent stability of the Cr-doped $LiNi_{0.5}Mn_{1.5}O_4$. That is why the charge and discharge capacities increase with increasing the charge voltage limit. In addition, the increase in charge and discharge capacities with the charge cutoff limit may also come from a small contribution of PF_6^- anion intercalation into and de-intercalation out of the conductive carbon SP which has some graphite-like layers. As seen in Fig. 11, the stabilized charge and discharge capacities of PF_6^- anions into and out of an SP-PVDF electrode increase with the cutoff voltage, from 2.5 mAh g^{-1} for 4.9 V, to 2.9 mAh g^{-1} for 5.0 V, 3.3 mAh g^{-1} for 5.1 V, 4.2 mAh g^{-1} for 5.2 V, and 6.4 mAh g^{-1} for 5.3 V. Considering that SP is only 10% of the whole electrode, the influence of SP is mainly on the initial irreversible capacity of the electrode (Fig. 7), and the capacity contribution of PF_6^- anions out of SP to the total discharge capacity of the spinel cathode is relatively small. The effect of "inactive" conductive carbon on the performance of high voltage cathode materials deserves further investigation.

On the other hand, when the charge voltage is set too high, e.g. 5.3 V, the carbonate solvents, especially DEC and EMC, are not stable and decompose significantly, causing rapid capacity fading. It should be noted that the gas generation from the decomposition of

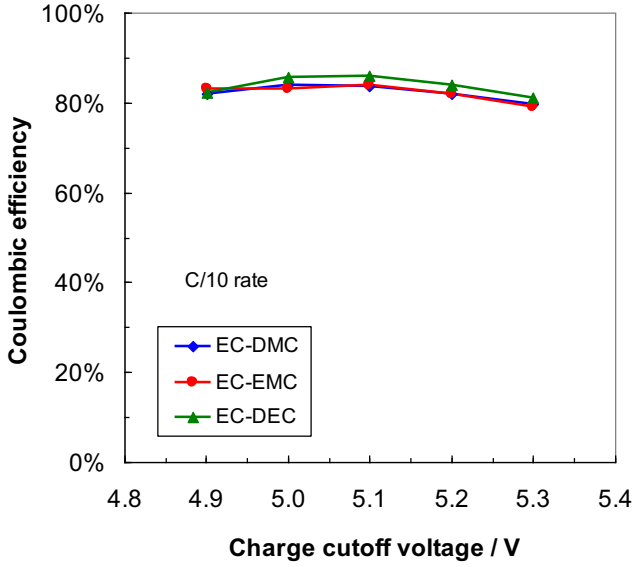

Fig. 6. Variation of the first-cycle Coulombic efficiency with the charge cutoff voltage for Li/$LiCr_{0.05}Ni_{0.45}Mn_{1.5}O_4$ half-cells using electrolyte of 1.0 M $LiPF_6$ in three carbonate mixtures.

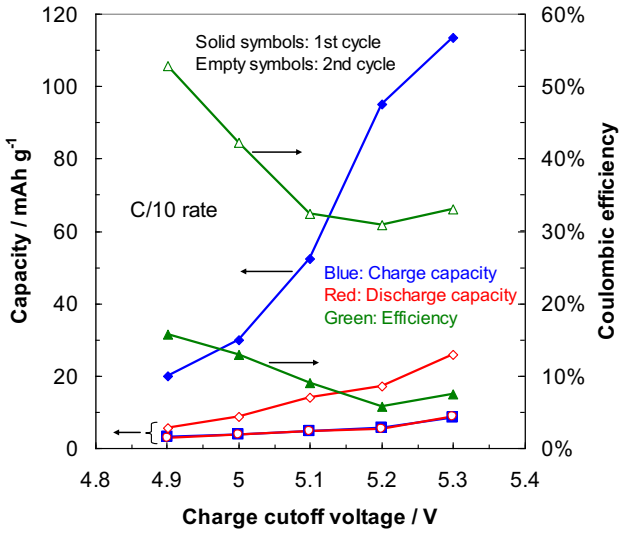

Fig. 7. Charge/discharge capacities and Coulombic efficiencies of Li/SP half-cells using electrolyte of 1.0 M $LiPF_6$ in EC-EMC mixture during the first and second cycles.

organic carbonate solvents on the cathode surface at high voltages also affects the cycling performance, as reported in many literature papers [44–47]. It is demonstrated that the three carbonate mixtures are stable to 5.2 V on the $LiCr_{0.05}Ni_{0.45}Mn_{1.5}O_4$ electrode. As for the cycling at 5.2 V, the capacity retention of the three carbonate mixtures is about 87% after 500 cycles at the 1C rate. Combined with the first-cycle efficiencies shown in Fig. 6, 5.2 V seems to be a critical cutoff voltage that delivers acceptable first-cycle efficiency and excellent long-term stability.

When comparing the three carbonate mixtures with respect to rate capabilities at different upper cutoff voltages (Fig. 12), it is seen that EC-DMC and EC-EMC have very similar rate performances, but EC-DEC has relatively inferior rate capability, especially at 5.3 V, indicating that EC-DEC is not suitable for high rate applications. This is mainly related to the lower ionic conductivity of EC-DEC electrolyte as compared to EC-DMC and EC-EMC, as shown in Table 1. Besides, the poor rate capability and poor cycling performance of EC-DEC at the high cutoff voltage of 5.3 V would also be ascribed to the relatively poor stability of EC-DEC at this high voltage.

The above results indicate that the stability of the electrolyte solvents depends strongly on the cathode materials used in the tests. For example, $LiCoO_2$ is well known to release lattice oxygen when

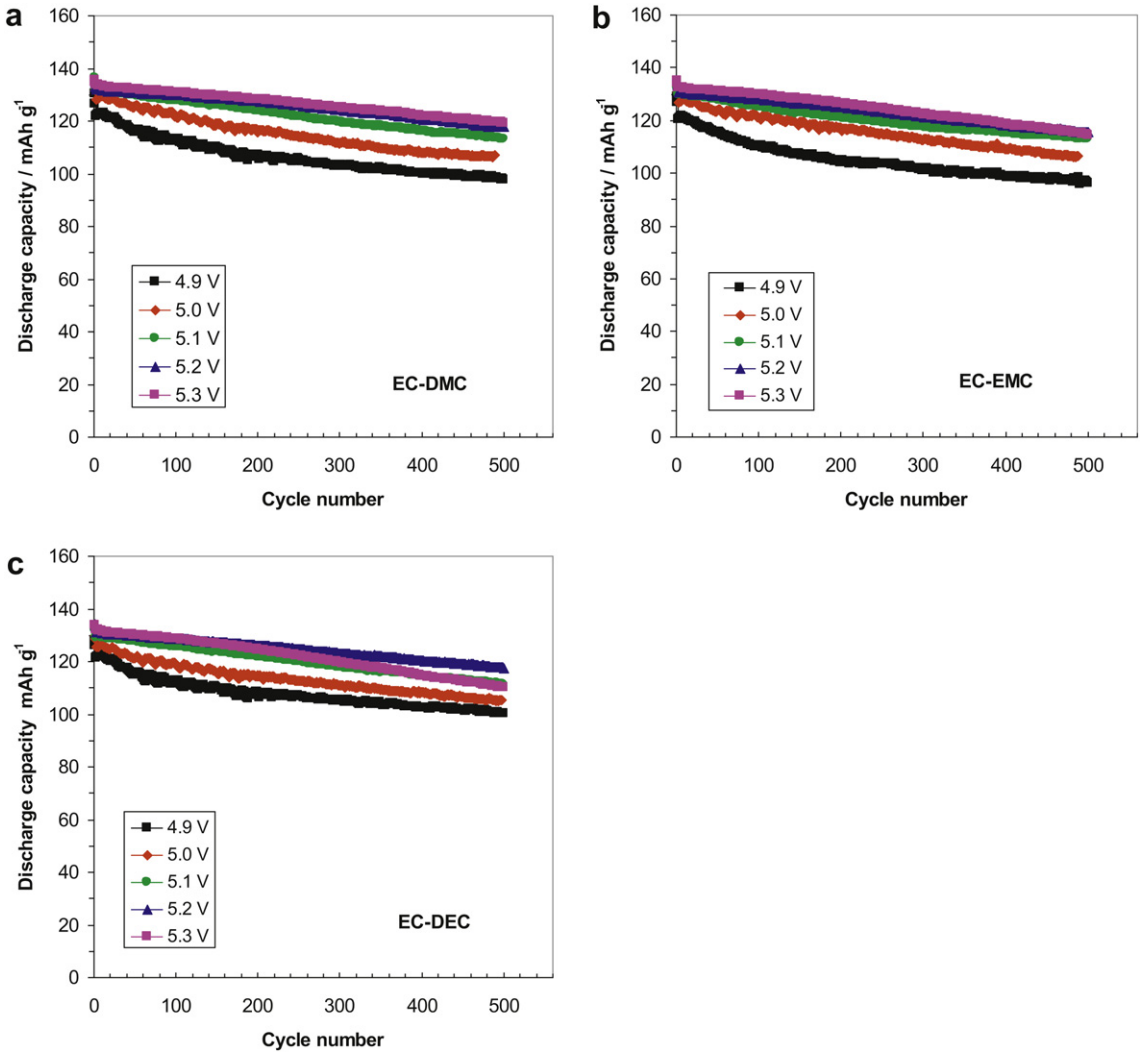

Fig. 8. Discharge capacities of Li/$LiCr_{0.05}Ni_{0.45}Mn_{1.5}O_4$ half-cells with electrolytes of 1.0 M $LiPF_6$ in three carbonate mixtures during long-term cycling at the 1C rate.

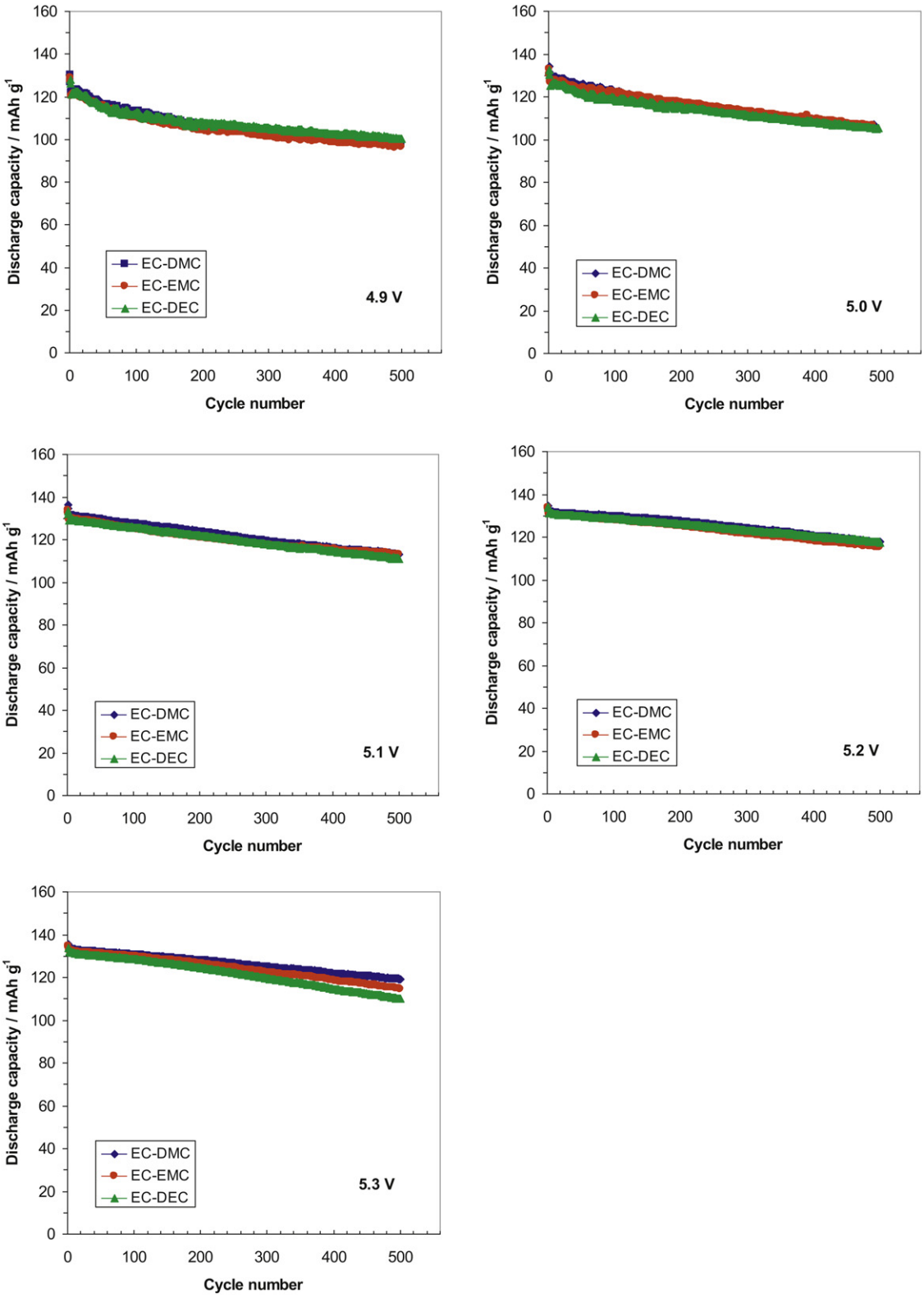

Fig. 9. Comparison of the long-term cycling performance of the Li/$LiCr_{0.05}Ni_{0.45}Mn_{1.5}O_4$ half-cells using three conventional carbonate electrolytes at different charge voltage limits.

charged to 4.3 V and above and the structure of its de-lithiated compound $Li_{1-x}CoO_2$ is not stable when $x > 0.5$ [48,49]. The released oxygen species can easily oxidize the carbonate solvents. In addition, Co compounds are known to have catalytic functions [50]. This is mainly attributed to the overlap between the t_{2g} band of Co^{3+}/Co^{4+} and the 2p band at the top of O^{2-}, which brings a significant amount of holes into the 2p band of O^{2-} at high voltage and results in the loss of oxygen from the electrode lattice [51]. Thus the carbonate

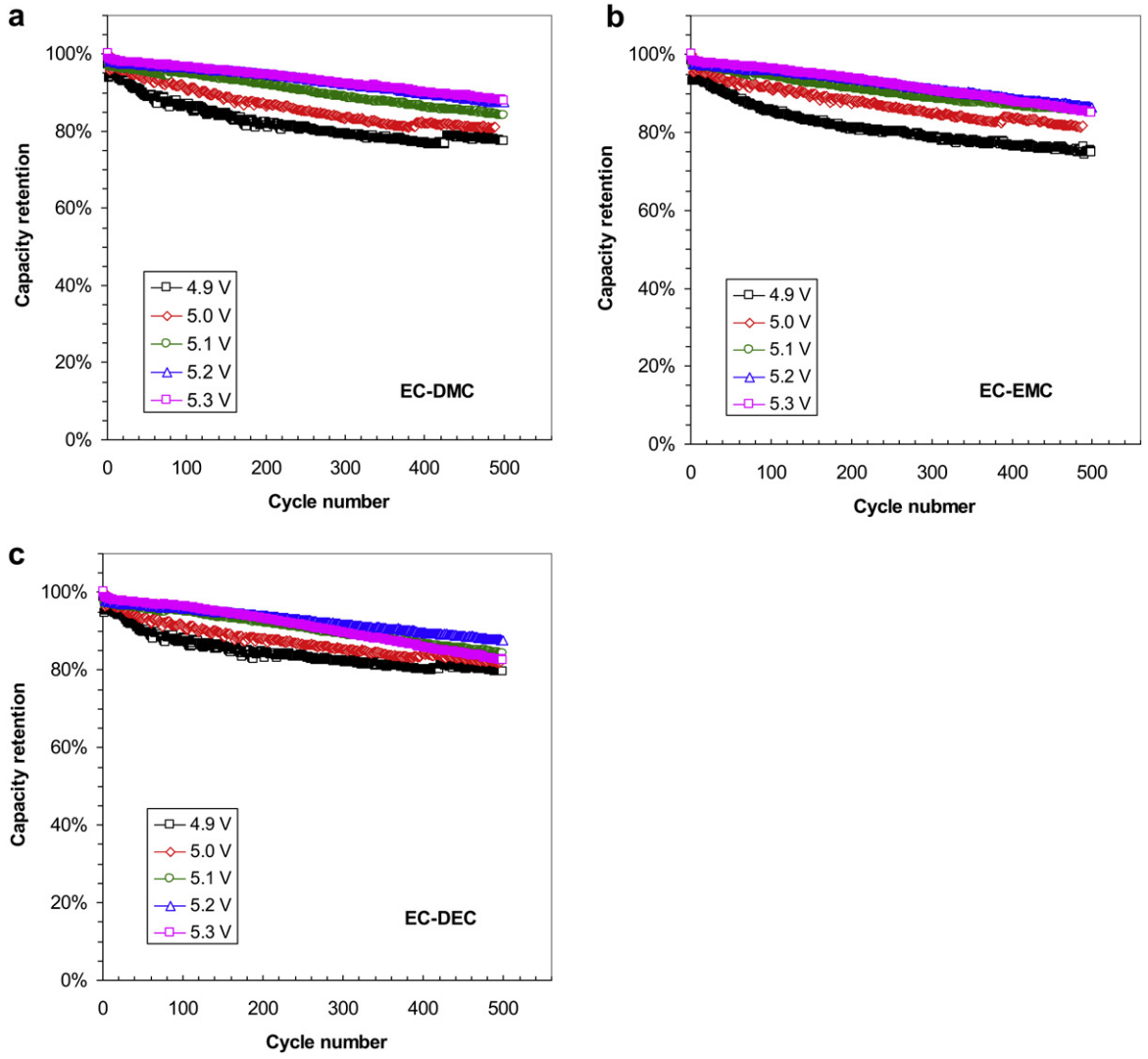

Fig. 10. Comparison of the capacity retention during long-term cycling of the Li/$LiCr_{0.05}Ni_{0.45}Mn_{1.5}O_4$ half-cells using three conventional carbonate electrolytes at different charge voltage limits.

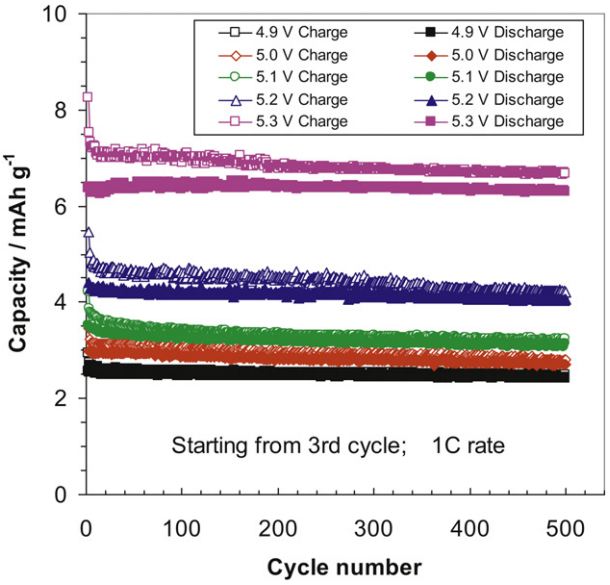

Fig. 11. Long-term cycling stability of Li/SP-PVDF half-cells using the electrolyte (1.0 M $LiPF_6$ in EC-EMC) at the 1C rate after the first two formation cycles at the C/10 rate.

solvents can also be decomposed by the catalytic Co compounds at high voltages. Similar situations may occur in the layered $LiNi_xMn_yCo_zO_2$ (where $x + y + z = 1$) and their lithium-rich cathode materials [52], $LiCoPO_4$ [53], and Li_2CoPO_4F [15,54]. The Li_2MnO_3-$LiNi_xMn_yCo_zO_2$ composite cathode materials have been reported to release oxygen during charge due to activation of Li_2MnO_3 [55]. $Li_3V_2(PO_4)_3$ has also been reported to have local structure change for PO_4^{3-} anions from crystalline to disordered phase after the third Li is removed [56]. It is seen that these high voltage cathode materials either release oxygen during charge (i.e. de-lithiation), or exhibit the catalytic functions of the transition metals and unstable structures after de-lithiation. All these factors contribute to the decomposition of electrolytes, especially the carbonate solvents, and rapidly decaying cycle life. It has been reported that surface modifications of the cathode active materials with non-reactive inorganic compounds can significantly improve their stability with conventional carbonate electrolytes at high voltages [57,58]. On the other hand, $LiNi_{0.5}Mn_{1.5}O_4$ and its doped cathode materials are quite stable in structure at high voltages [59]. These spinel cathode materials show excellent compatibility with carbonate electrolytes. Therefore, it is believed that once the active cathode materials are stable, carbonate electrolytes can be cycled up to at least 5.2 V for long cycle life.

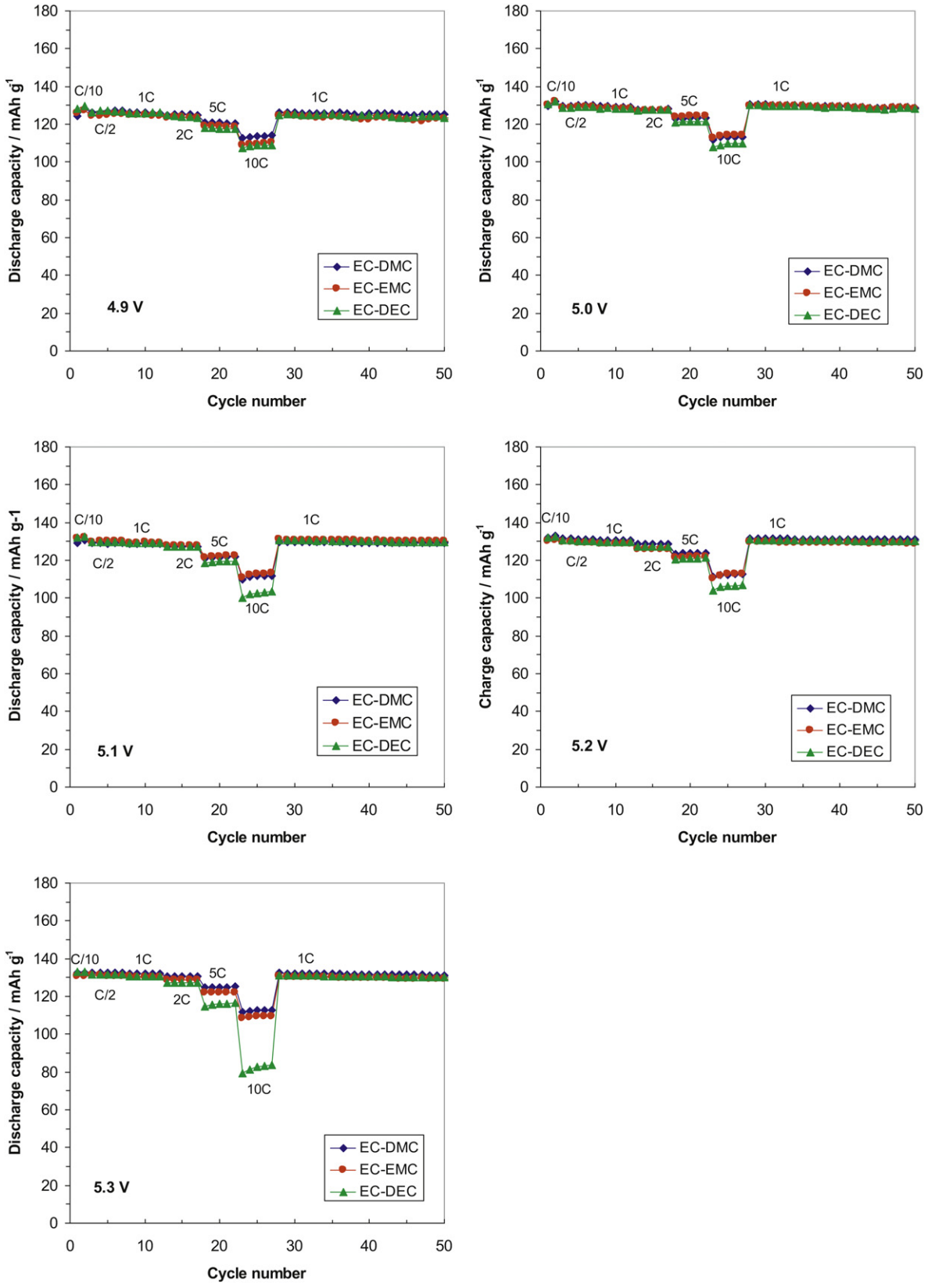

Fig. 12. Comparison of the rate performance of the Li/$LiCr_{0.05}Ni_{0.45}Mn_{1.5}O_4$ half-cells using three conventional carbonate electrolytes at different charge voltage limits.

4. Conclusions

The charge voltage limits of single- and mixed-carbonate solvents in Li-ion batteries have been systematically investigated in lithium half-cells using stable cathode material of Cr-doped $LiNi_{0.5}Mn_{1.5}O_4$. We have found that the conventional electrolytes based on EC and linear carbonate mixtures have very similar long-term cycling performance (up to 500 cycles) in half-cells when they are cycled up to 5.2 V. The discharge capacity increases with the charge cutoff voltage and reaches the best capacity retention at 5.2 V. The first-cycle efficiency has a maximum value at 5.1 V for all three carbonate mixtures studied. EC-DMC and EC-EMC have similar rate capacities and better rate performance than EC-DEC, indicating that EC-DEC is not suitable for high rate applications. Even when cycled at 5.3 V, EC-DMC still demonstrated good cycling performance while EC-EMC and EC-DEC showed a little faster capacity fading. Therefore, the electrochemical stability of carbonate electrolytes is strongly related to the cathode active materials and the interactions among them. With a stable cathode material such as Cr-doped $LiNi_{0.5}Mn_{1.5}O_4$, the conventional carbonate electrolytes can be long-term cycled up to at least 5.2 V.

Acknowledgments

This work was sponsored by the Laboratory Directed Research and Development Project of Pacific Northwest National Laboratory and by the Assistant Secretary for Energy Efficiency and Renewable Energy, Office of Vehicle Technologies of the U.S. Department of Energy under Contract No. DE-AC02-05CH11231, Subcontract No 18769, under the Batteries for Advanced Transportation Technologies (BATT) Program. Pacific Northwest National Laboratory (PNNL) is operated by Battelle for the U.S. Department of Energy under contract No. DE-AC05-76RL01830.

References

[1] Y. Li, Z. Zhou, M. Ren, X. Gao, J. Yan, Electrochim. Acta 51 (2006) 6498.
[2] Q. Chen, J. Wang, Z. Tang, W. He, H. Shao, J. Zhang, Electrochim. Acta 52 (2007) 5251.
[3] R. Santhanam, B. Rambabu, J. Power Sources 195 (2010) 5442.
[4] K.M. Shaju, P.G. Bruce, Dalton Trans. (2008) 5471.
[5] T.A. Arunkumar, A. Manthiram, Electrochim. Acta 50 (2005) 5568.
[6] G.Q. Liu, W.S. Yuan, G.Y. Liu, Y.W. Tian, J. Alloys Compds 484 (2009) 567.
[7] Y.-K. Sun, K.-J. Hong, J. Prakash, K. Amine, Electrochem. Commun. 4 (2002) 344.
[8] D.W. Shin, A. Manthiram, Electrochem. Commun. 13 (2011) 1213.
[9] G.B. Zhong, Y.Y. Wang, Z.C. Zhang, C.H. Chen, Electrochim. Acta 56 (2011) 6554.
[10] X. Zhang, H. Zheng, V. Battaglia, R.L. Axelbaum, Proc. Combust. Inst. 33 (2011) 1867.
[11] M.E. Rabanal, M.C. Gutierrez, F. Garcia-Alvarado, E.C. Gonzalo, M.E. Arroyo-de Dompablo, J. Power Sources 160 (2006) 523.
[12] B. Jin, H.-B. Gu, K.-W. Kim, J. Solid State Electrochem 12 (2008) 105.
[13] J.L. Shui, Y. Yu, X.F. Yang, C.H. Chen, Electrochem. Commun. 8 (2006) 1087.
[14] E. Dumont-Botto, C. Bourbon, S. Patoux, P. Rozier, M. Dolle, J. Power Sources 196 (2011) 2274.
[15] D. Wang, J. Xiao, W. Xu, Z. Nie, C. Wang, G.L. Graff, J.-G. Zhang, J. Power Sources 196 (2011) 2241.
[16] K. Xu, C.A. Angell, J. Electrochem. Soc. 145 (1998) L70.
[17] K. Xu, Chem. Rev. 104 (2004) 4303.
[18] M. Moshkovich, M. Cojocaru, H.E. Gottlieb, D. Aurbach, J. Electroanal. Chem. 497 (2001) 84.
[19] K. Kanamura, J. Power Sources 81-82 (1999) 123.
[20] K. Kanamura, S. Toriyama, S. Shiraishi, Z. Takehara, J. Electrochem. Soc. 143 (1996) 2548.
[21] J. Liu, A. Manthiram, Chem. Mater. 21 (2009) 1695.
[22] J. Liu, A. Manthiram, J. Phys. Chem. C 13 (2009) 15073.
[23] J. Xiao, X. Chen, P.V. Sushko, M.L. Sushko, L. Kovarik, J. Feng, Z. Deng, J. Zheng, G.L. Graff, Z. Nie, D. Choi, J. Liu, J.-G. Zhang, M.S. Whittingham, Adv. Mater. 24 (2012) 2109.
[24] W. Xu, J. Xiao, J. Zhang, D. Wang, J.-G. Zhang, J. Electrochem. Soc. 156 (2009) A773.
[25] W. Xu, N.L. Canfield, D. Wang, J. Xiao, Z. Nie, X.S. Li, W.D. Bennett, C.C. Bonham, J.-G. Zhang, J. Electrochem. Soc. 157 (2010) A765.
[26] A.D. Becke, Phys. Rev. A 38 (1988) 3098.
[27] J.P. Perdew, Phys. Rev. B 33 (1986) 8822.
[28] C. Lee, W. Yang, R.G. Parr, Phys. Rev. B 37 (1988) 785.
[29] B. Miehlich, A. Savin, H. Stoll, H. Preuss, Chem. Phys. Lett. 157 (1989) 200.
[30] A.D. Becke, J. Chem. Phys. 98 (1993) 5648.
[31] W. Xu, A. Read, P.K. Koech, D. Hu, C. Wang, J. Xiao, A.B. Padmaperuma, G.L. Graff, J. Liu, J.-G. Zhang, J. Mater. Chem. 22 (2012) 4032.
[32] Z. Zhang, M.M. Lerner, J. Electrochem. Soc. 140 (1993) 742.
[33] R.T. Carlin, H.C. De Long, J. Fuller, P.C. Trulove, J. Electrochem. Soc. 141 (1994) L73.
[34] J.A. Seel, J.R. Dahn, J. Electrochem. Soc. 147 (2000) 892.
[35] T. Ishihara, M. Koga, H. Matsumoto, M. Yoshio, Electrochem. Solid-State Lett. 10 (2007) A74.
[36] W.C. West, J.F. Whitacre, N. Leifer, S. Greenbaum, M. Smart, R. Bugga, M. Blanco, S.R. Narayanan, J. Electrochem. Soc. 154 (2007) A929.
[37] K. Takahashi, M. Saitoh, M. Sano, M. Fujita, K. Kifune, J. Electrochem. Soc. 151 (2004) A173.
[38] K. Ariyoshi, Y. Iwakoshi, N. Nakayama, T. Ohzuku, J. Electrochem. Soc. 151 (2004) A296.
[39] J.H. Kim, C.S. Yoon, S.T. Myung, J. Prakash, Y.K. Sun, Electrochem. Solid-State Lett. 7 (2004) A216.
[40] J.-H. Kim, S.-T. Myung, C.S. Yoon, S.G. Kang, Y.-K. Sun, Chem. Mater. 16 (2004) 906.
[41] M. Kunduraci, G.G. Amatucci, J. Electrochem. Soc. 153 (2006) A1345.
[42] M. Kunduraci, J.F. Al-Sharab, G.G. Amatucci, Chem. Mater. 18 (2006) 3585.
[43] S. Patoux, L. Sannier, H. Lignier, Y. Reynier, C. Bourbon, S. Jouanneau, F.L. Cras, S. Martinet, Electrochim. Acta 53 (2008) 4137.
[44] W. Kong, H. Li, X. Huang, L. Chen, J. Power Sources 142 (2005) 285.
[45] M. Holzapfel, A. Würsig, W. Scheifele, J. Vetter, P. Novák, J. Power Sources 174 (2007) 1156.
[46] M. Onuki, S. Kinoshita, Y. Sakata, M. Yanagidate, Y. Otake, M. Ue, M. Deguchi, J. Electrochem. Soc. 155 (2008) A794.
[47] J.H. Seo, J. Park, G. Plett, A.M. Sastry, Electrochem. Solid-State Lett. 13 (2010) A135.
[48] J.-M. Tarascon, M. Armand, Nature 414 (2001) 359.
[49] D.G. Kellerman, V.V. Karelina, V.S. Gorshkov, Y. Blinovskov, Chem. Sustain. Devel 10 (2002) 721.
[50] A. Débart, J. Bao, G. Armstrong, P.G. Bruce, J. Power Sources 174 (2007) 1177.
[51] R.V. Chebiam, A.M. Kannan, F. Prado, A. Manthiram, Electrochem. Commun. 3 (2001) 624.
[52] T.A. Arunkumar, Y. Wu, A. Manthiram, Chem. Mater. 19 (2007) 3067.
[53] L. Tan, Z. Luo, H. Liu, Y. Yu, J. Alloys Compd. 52 (2010) 407.
[54] S. Okada, M. Ueno, Y. Uebou, J.-I. Yamaki, J. Power Sources 146 (2005) 565.
[55] N. Yabuuchi, K. Yoshii, S.-T. Myung, I. Nakai, S. Komaba, J. Am. Chem. Soc. 133 (2011) 4404.
[56] C.M. Burba, R. Frech, Solid State Ionics 177 (2007) 3445.
[57] J.M. Zheng, Z.R. Zhang, X.B. Wu, Z.X. Dong, Z. Zhu, Y. Yang, J. Electrochem. Soc. 155 (2008) A775.
[58] H.M. Wu, I. Belharouak, A. Abouimrane, Y.-K. Sun, K. Amine, J. Power Sources 195 (2010) 2909.
[59] G.B. Zhong, Y.Y. Wang, Y.Q. Yu, C.H. Chen, J. Power Sources 205 (2012) 385.